

Supplementary Information

Characterization and Implications of Solids Associated with Hydraulic Fracturing Flowback and
Produced Water from the Duvernay Formation, Alberta, Canada

Shannon L. Flynn^{1,2*}, Konstantin von Gunten², Tyler Warchola², Katherine Snihur², Tori Z.
Forbes³, Greg G. Goss⁴, Murray K. Gingras², Kurt O. Konhauser², and Daniel S. Alessi².

¹School of Natural and Environmental Sciences,

Newcastle University, Newcastle upon Tyne, NE1 7RU, UK

²Department of Earth and Atmospheric Sciences,

University of Alberta, Edmonton, AB T6G 2E3, Canada

³Department of Chemistry

University of Iowa, Iowa City, IA, 52242, USA

⁴Department of Biological Sciences,

University of Alberta, Edmonton, AB T6G 2E3, Canada

** Corresponding Author: shannon.flynn@ncl.ac.uk*

Duvernay Formation Geology and Composition

The Frasnian Duvernay Formation (Woodbend Group) is a bituminous and variably calcareous mudstone that is present throughout most of the Western Canada Sedimentary Basin. The Duvernay Formation is laterally equivalent to the Leduc Formation, a carbonate platform and reef complex that has been exploited for conventional oil and gas since 1947. The Geology of the Duvernay Formation is summarized in Stoakes¹. The Duvernay Formation comprises interbedded bituminous shales, dark brown, calcareous shales and dense argillaceous limestones. More rarely observed are fossil-rich lime mud accumulations. The bituminous shales are characteristically plane-parallel laminated. Argillites are also planar laminated, but may also be massive appearing or completely bioturbated. The variability in bedding is best interpreted as unsteadiness in oxygenation further suggesting that redox-sensitive elements are heterogeneously distributed. The shales and the argillites contain — in descending abundance — silt-sized quartz, mica, K-feldspar, and plagioclase; the clay-size fraction is dominantly quartz and calcite with subordinate clay illite/smectite and less abundant kaolinite^{2,3}. Total organic content is variable, locally exceeding 10% and more commonly between 1 and 3%⁴. Eogenetic to diagenetic pyrite is locally common. Barite, likely from hydrothermal sources, is present up to 1.4 weight %³.

Profile of Well 3

Well 3 was drilled into the Duvernay Formation at a depth of 3172 m with a horizontal bore length of 2535. Sample A came from 139 m into the horizontal bore while B came from 839 m (Figure SI.1)

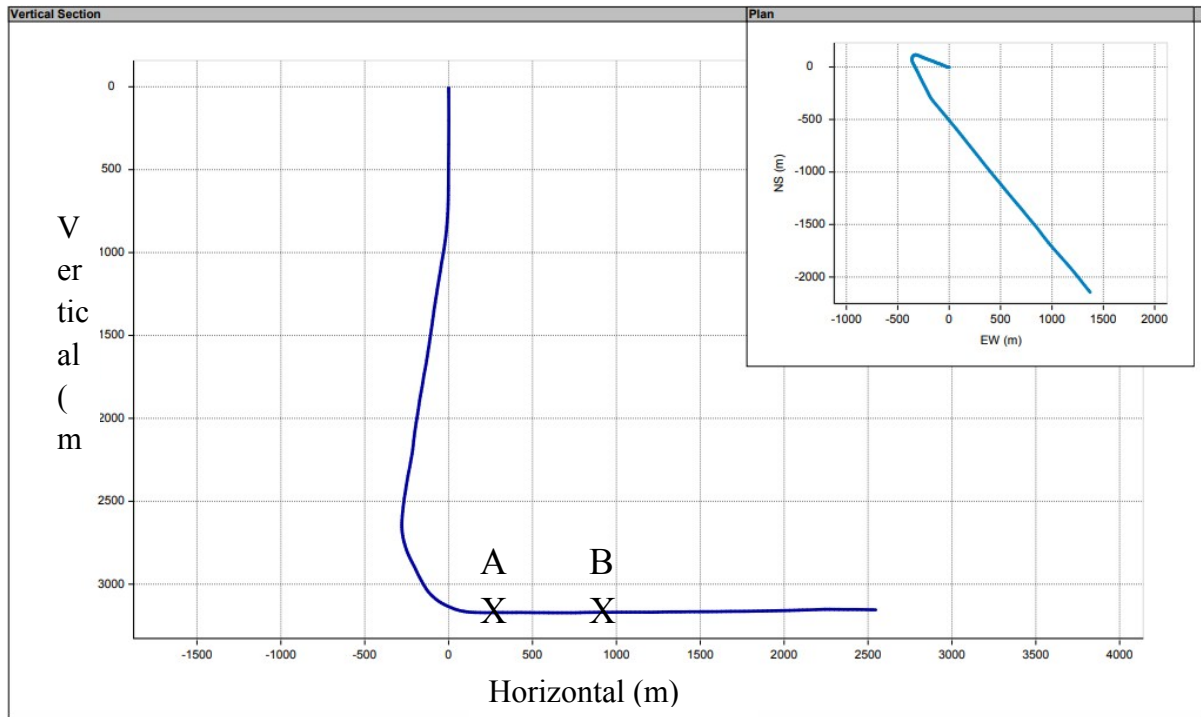


Figure SI.1 Schematic of well 3's bore showing the approximate locations from where drill cutting samples A and B were obtained.

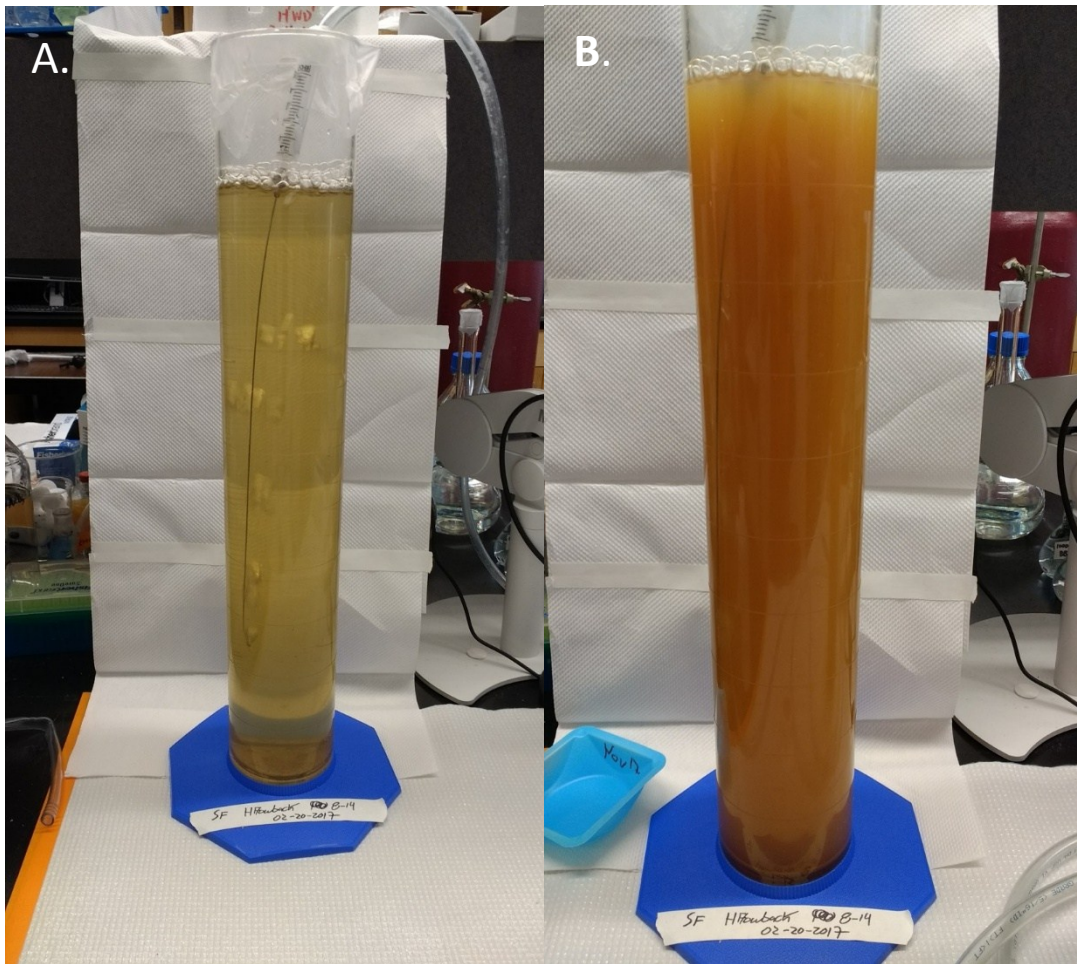


Figure SI.2 Sample S3 before (A) and after bubbling (B).

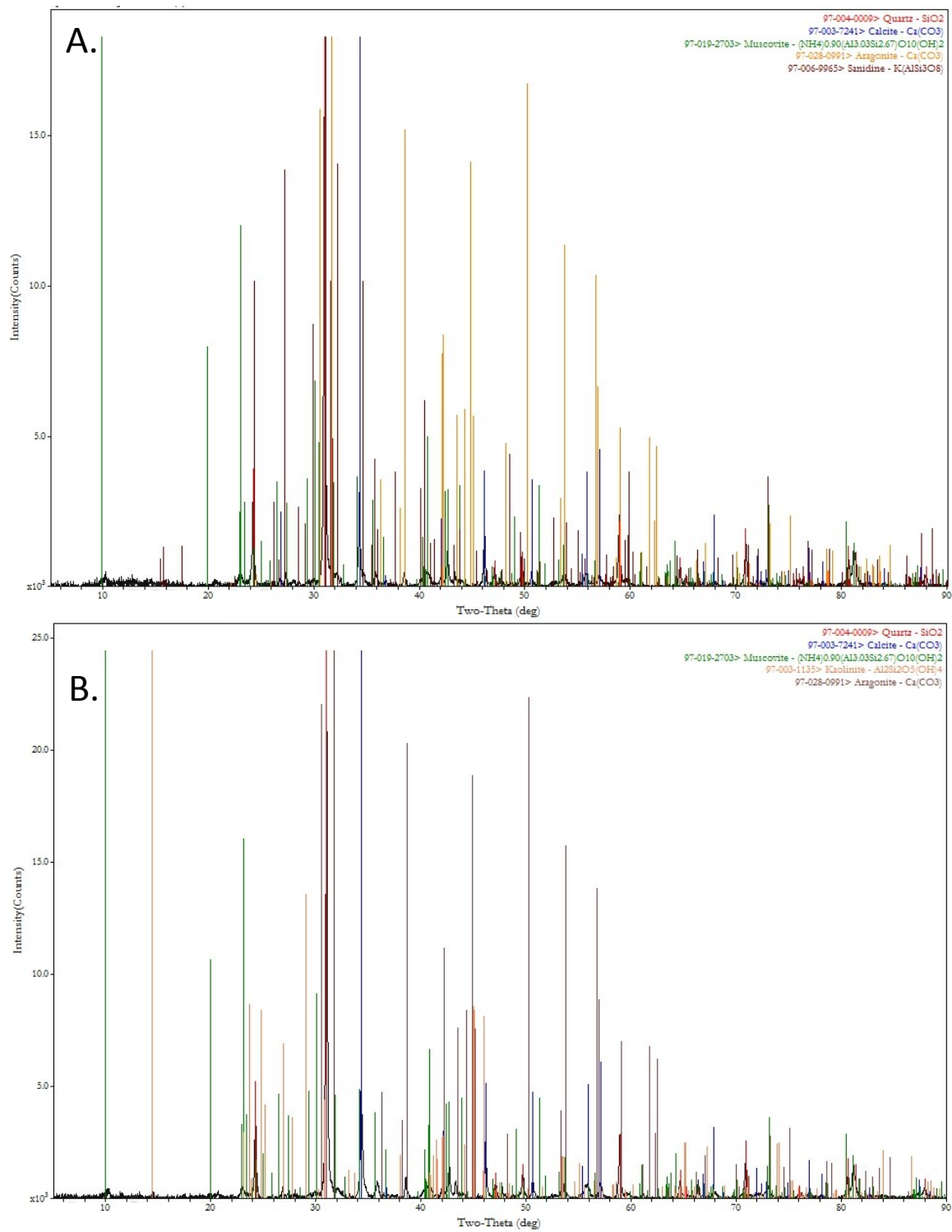


Figure SI.3 XRD spectra of the bulk mineralogy from drill cuttings from well 3's lateral bore A) 3550 m and B) 4250 m.

Table SI.1 The elemental composition of the FPW associated solids in mM as determined by alkaline fusion digestions and the associated relative standard deviation (RSD) as determined through three replicate digestions.

Element	S1	RSD	S2	RSD	S3	RSD	S3 Ox	RSD
	mM	%	mM	%	mM	%	mM	%
Mg	0.757	4.5	12.0	17.5	29.5	5.5	7.53	24.9
Al	10.7	30.0	96.9	3.8	57.0	8.8	2.17	37.2
Si	3,350	4.9	5,810	3.0	4,040	5.2	1,420	13.5
P	10.6	20.5	3.72	77.0	35.2	9.9	11.9	51.8
S	322	4.8	778	3.8	851	6.7	73.1	20.4
K	17.9	14.4	43.3	5.7	45.7	10.2	2.77	57.5
Ca	99.7	2.4	139	6.1	634	5.0	370	15.1
Mn	NM		1.74	3.9	NM		0.834	16.2
Fe	5,890	4.5	1,630	5.4	3,010	4.2	3,480	15.2
Zn	NM		2.44	46.6	NM		1.56	25.7
Sr	121	3.8	717	2.4	330	6.1	44.3	18.0
Ba	166	4.4	49.0	6.3	468	6.3	43.5	20.3

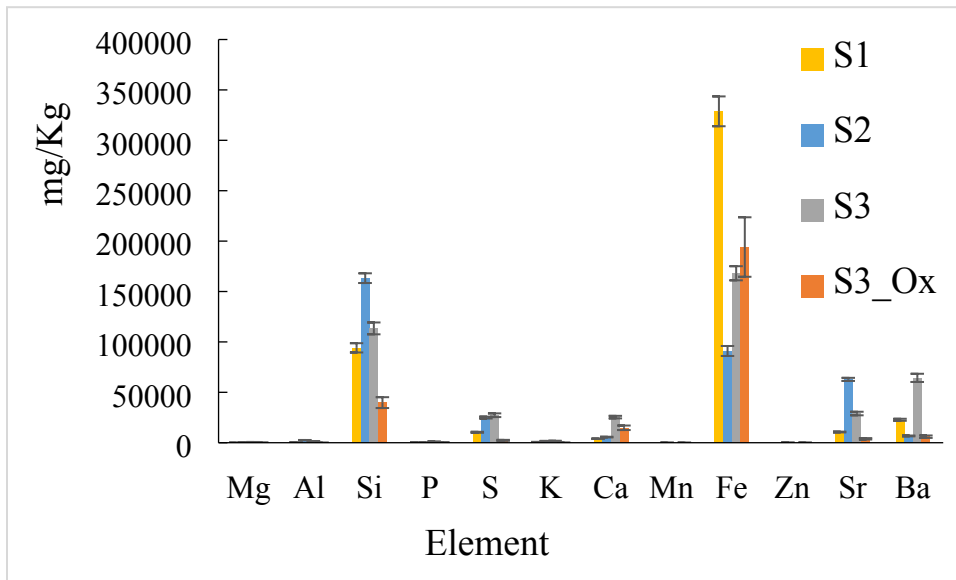


Figure SI.4 Elemental profile of FPW solids as determined through alkaline fusion digestion, in which the error bars represent ± 1 standard deviation.

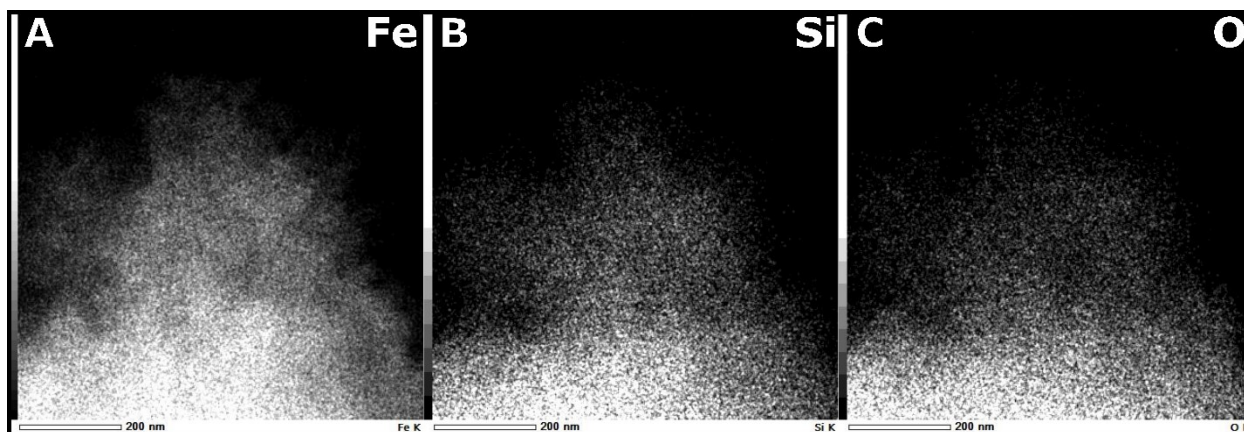


Figure SI.5 STEM elemental maps of particle agglomerates from S1 showing the distribution of A) Fe, B) Si, and C) O.

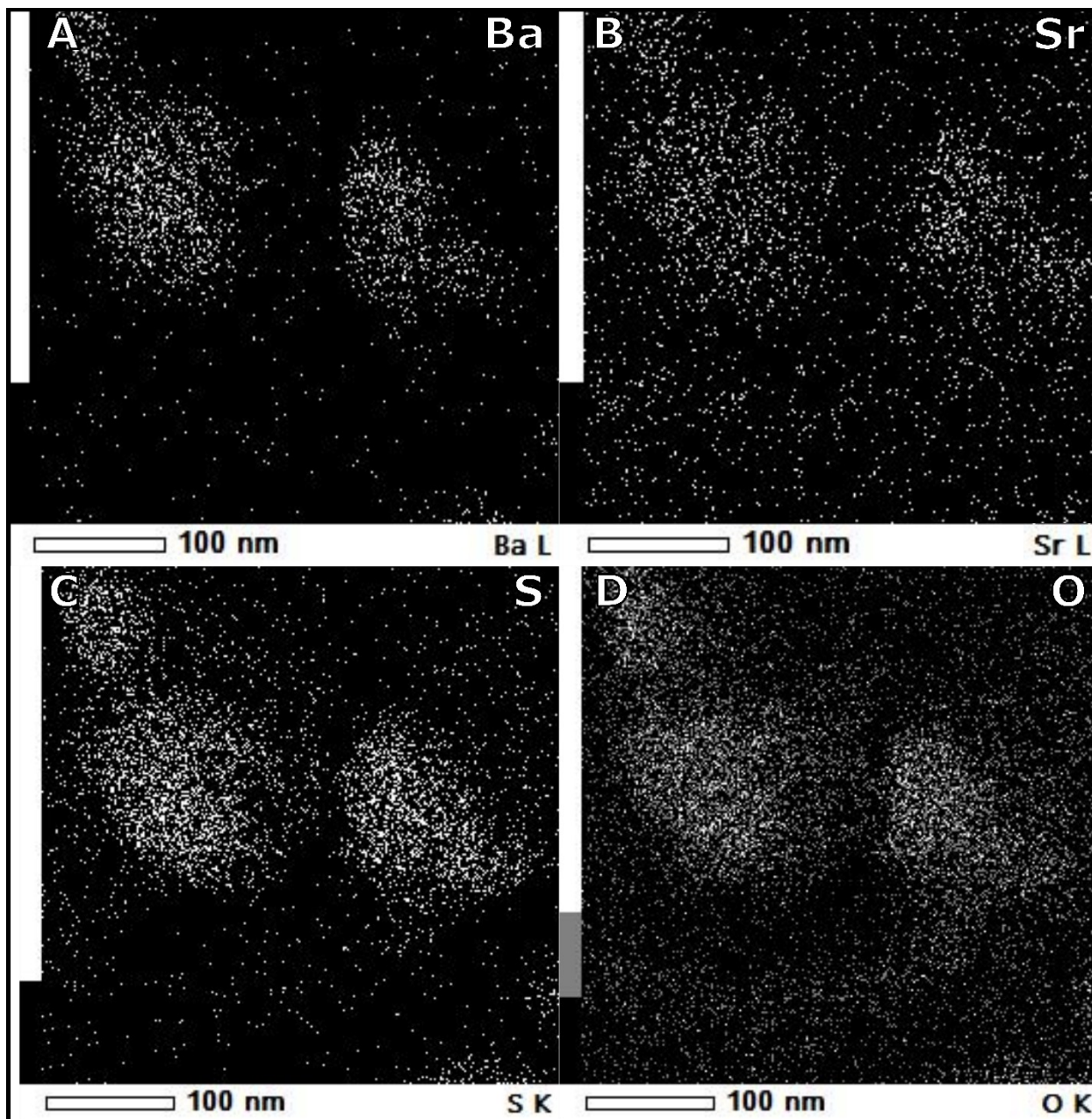


Figure SI.6 STEM elemental maps of particle agglomerates from S1 showing the distribution of A) Ba, B) Sr, C) S, and D) O.

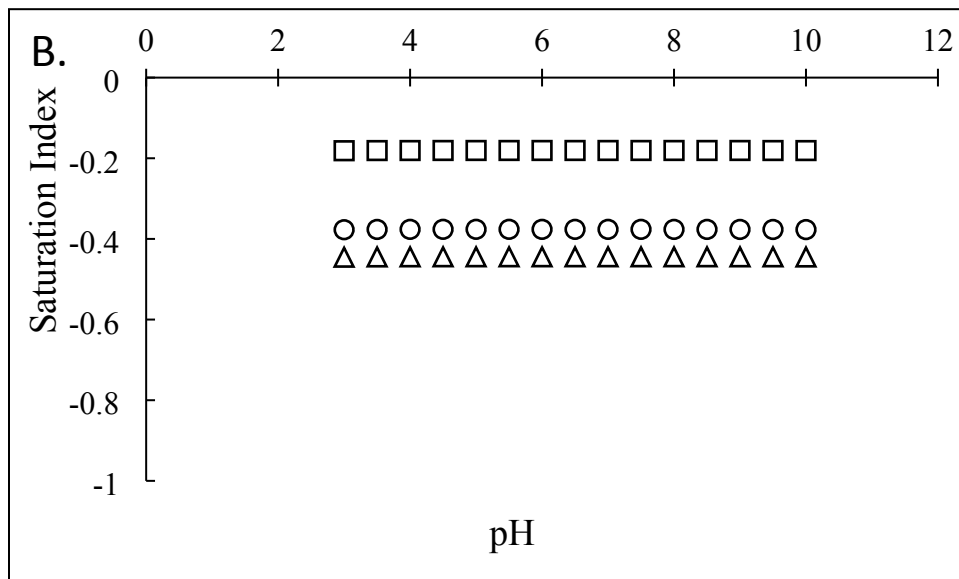
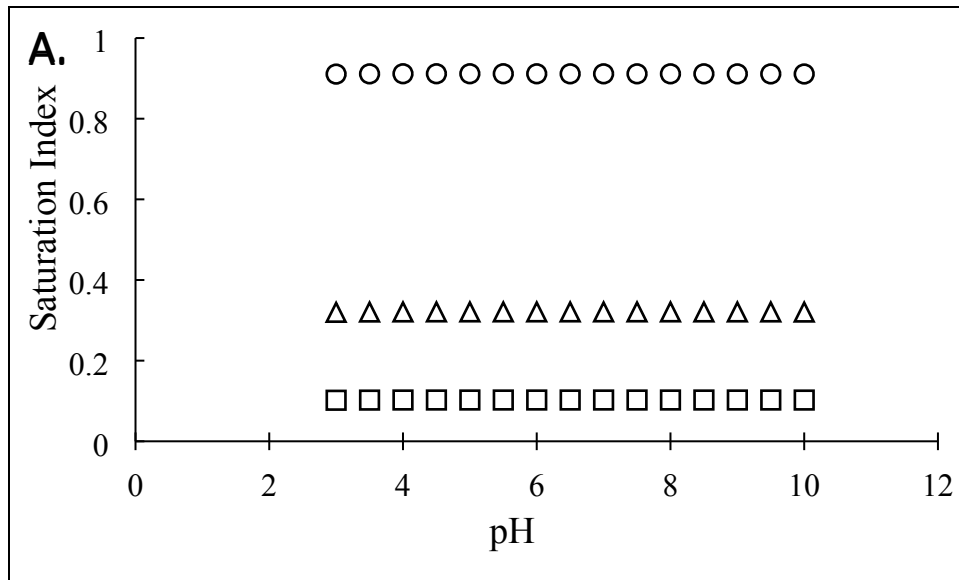


Figure SI.7 Saturation indices (SI) of hypothesized minerals present FPW modeled using the element data as a function of pH A) respect to barite, and B) celestine, with S1, S2, and S3 represented by (□), (Δ), and (○), respectively.

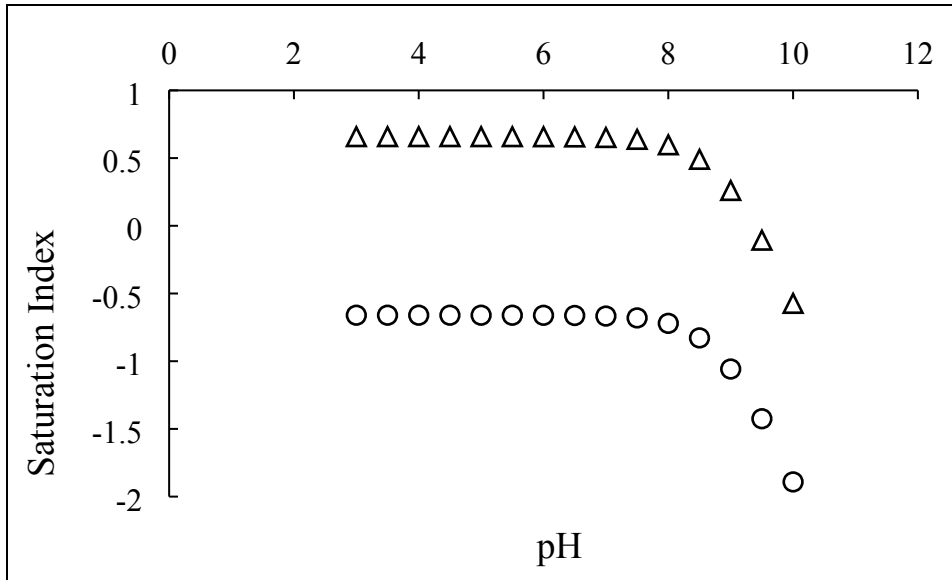


Figure SI.8 Saturation indices (SI) of potential silicate minerals present in FPW modeled using the element data from S1 as a function of pH for $\text{SiO}_{2(\text{am})}$ (□), and quartz (Δ).

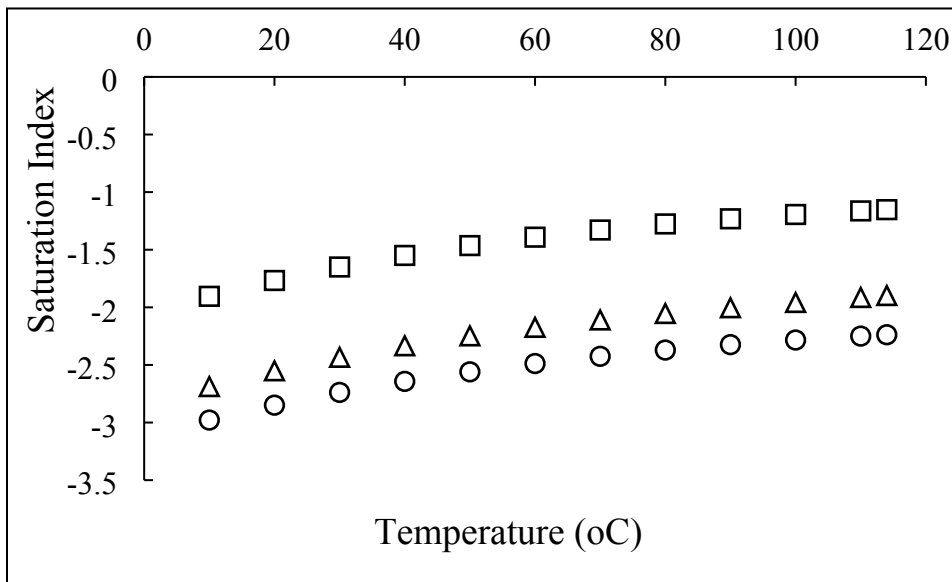
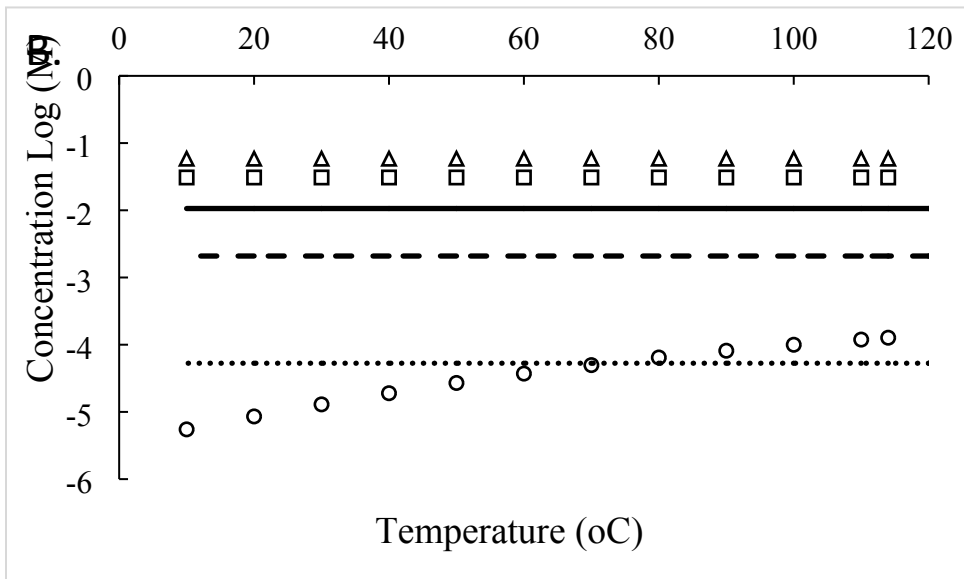
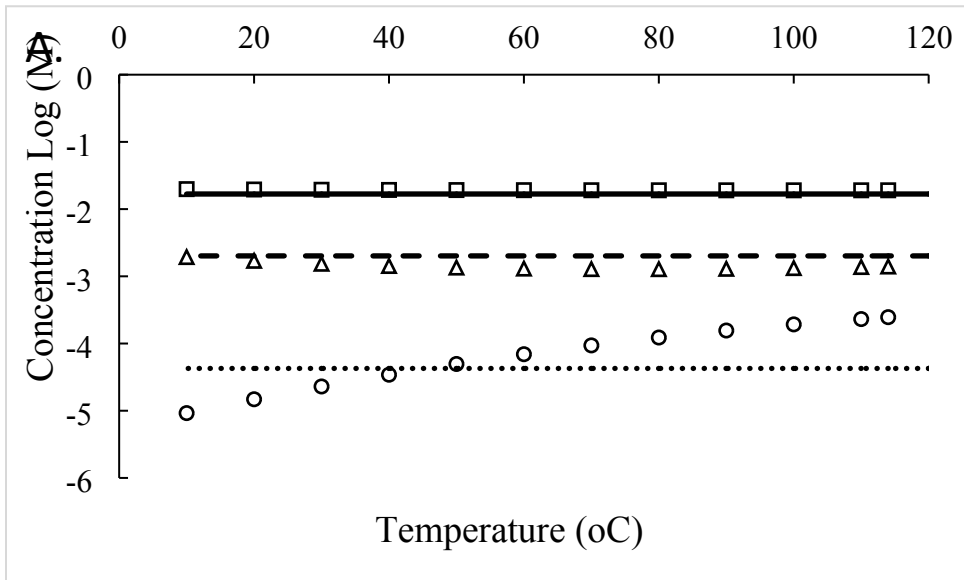


Figure SI.9 Saturation indices (SI) of CO_2 modeled using the FPW chemistry as a function of temperature with samples S1, S2, and S3 represented by (□), (Δ), and (○), respectively.



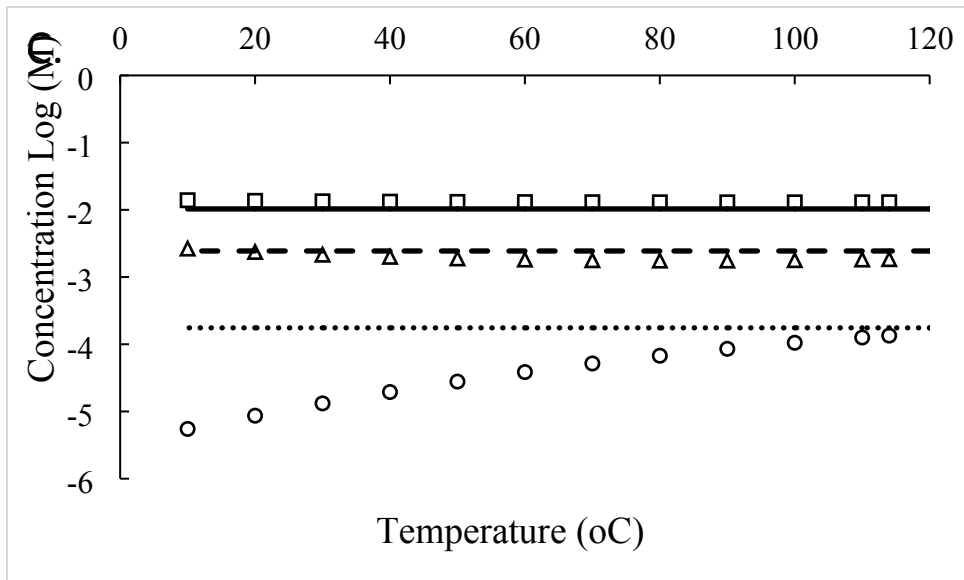


Figure SI.10 Comparison of the measured and model elemental concentrations in equilibrium with celestine and barite for A) S1, B) S2, and S3 in which the modeled Sr concentration is represented by (□), SO₄²⁻ by (Δ), and by Ba (○). The measured concentrations are for Sr, S, and Ba, represented by the solid, dashed and dotted lines respectively.

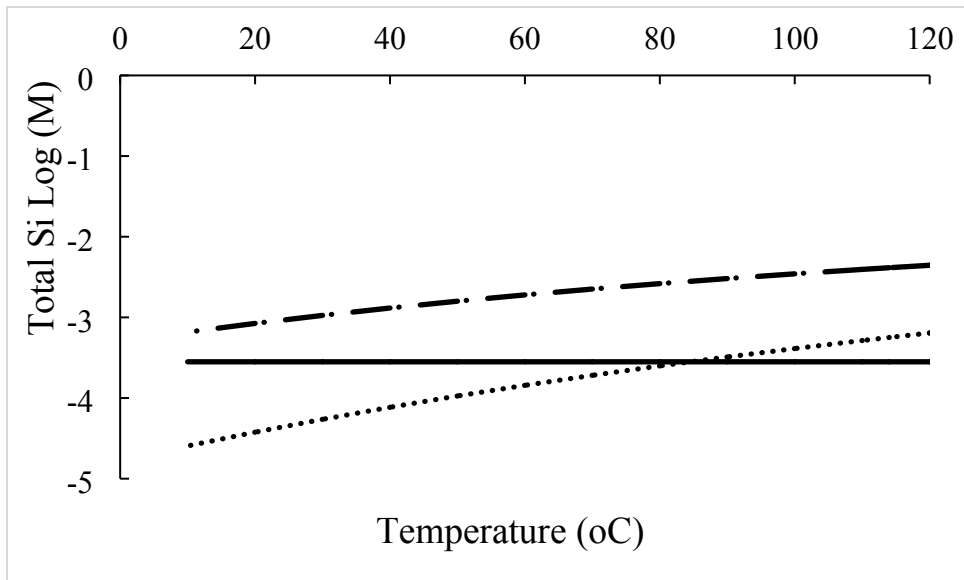


Figure SI.11 Comparison of the measured and model elemental concentrations of Si for S1 in equilibrium with silica minerals quartz and SiO_{2(am)} as a function of cooling temperatures. The modeled concentrations of Si in equilibrium with quartz and SiO_{2(a)} are represented by the dotted, and dotted and dashed lines, respectively. The solid line represents the measured Si concentration for S1.

Table SI.2 Data used to model the SI for barite (BaSO₄), celestine (SrSO₄), quartz (SiO₂), and amorphous silica (SiO_{2(am)}) using FPW data from the Fayetteville, Bakken, Denver-Julesburg, Marcellus and Barnett Formations. NR denotes not reported and ND denotes not detected.

		Ba	Br	Alkalinity as CO ₃ ²⁻	Ca	Cl	Fe	K	Mg	Mn	Na	SO ₄ ²⁻	Si	Sr	pH
Fayetteville	Site	(ppm)	(ppm)	(ppm)	(ppm)	(ppm)	(ppm)	(ppm)	(ppm)	(ppm)	(ppm)	(ppm)	(ppm)	(ppm)	
Warner et al. ⁵	FS-1	5	96	1,136.6	221	5507	1	NR	56	2	3,232	ND	47	27	NR
	FS-2	4	122	486.0	345	10,165	13	NR	61	2	3,575	ND	13	14	NR
	FS-3	4	144	538.4	350	9,896	10	NR	75	3	4,607	ND	22	49	NR
	FS-4	3	101	874.6	386	10,312	1	NR	67	2	4,224	3	160	18	NR
	FS-5	3	97	800.0	284	6,771	8	NR	47	2	3,152	ND	18	26	NR
Bakken															
Shrestha et al. ⁶	PW1	9.2	558	17.5	12,033	119,989	19.2	NR	1001	16.7	47,217	128	NR	774	NR
	PW2	12.4	384	84.5	8,573	75,892	30.2	NR	741	13.1	34,745	102	NR	551	NR
	PW3	26.3	91.6	428	372	21,728	0.7	NR	118	0.2	12,271	NR	NR	33.1	NR
	PW4	6.4	601	NR	15,346	136,220	22.3	NR	1299	15.8	60,571	293	NR	970	NR
	FW1	10.5	NR	145.35	9,683.3	118,666	96	NR	1273.3	7.1	61,466	650	NR	764	NR
Denver-Julesburg															
Rosenblum et al. ⁷²	HF	41.39	191.6	235.04	550	17,497	2.71	51.6	71.4	1.03	10,461	8.5	31.96	78	6.84

	VF1	41.07	244.4	41.97	1,081	24,955	6	75.9	119.3	0.19	14,215	>0.05	42	179	6.59	
	VF2	31.55	265.1	67.15	1,204	27,103	4.8	65.4	130	0.33	14,794	>0.05	29	202	6.93	
	VF3	14.15	81.3	164.88	365.5	12,724	19	52.9	40.5	0.29	7472	26.63	41	47	6.93	
Marcellus																
Haluszczak et al. ⁸		11,990	872	42.6	11,200	98,300	747	281	875	5.6	36,400	50	NR	2,330	6.2	
Barbot et al. ⁹		2,224	511	99	7,220	57,447	40.8	0	632	0	24,123	71	NR	1,695	6.56	
He et al. ¹⁰	A	730	NR	NR	2,170	29,000	NR	NR	249	NR	11,860	NR	NR	362	7.42	
	B	236	NR	NR	15,021	104,300	NR	NR	1720	NR	27,946	14.8	NR	1799	6.4	
Barnett																
Hayes and Severin ¹¹		3.6	589	441	1,600	34,700	24.9	316	255	0.86	18,850	709	NR	529	7.05	

Warner et al.⁵: 5 Flowback water samples from the Fayetteville Formation.

Shrestha et al.⁶: 4 produced water and 1 flowback sample from the Bakken Formation.

Rosenblum et al.⁷: 4 total flowback samples, 1 from a horizontally fractured well and 3 from vertically fractured well from the Wattenberg field in the Denver-Julesburg Basin.

Haluszczak et al.⁸: median concentration from day 14 flowback from 7 wells in the Marcellus Formation.

Barbot et al.⁹: average from 95 Marcellus flowback samples.

He et al.¹⁰: two composite samples from separate wells in the Marcellus Formation. Sample A is a composite of days 1, 5 and 7, while sample B is a composite of FPW from days 1, 3, and 5.

Hayes and Severin¹¹: the median of samples from 4 wells in the Barnett Formation from days 10-12.

References

- (1) F.A. Stoakes, Nature and control of shale basin fill and its effect on reef growth and termination: Upper Devonian Duvernay and Ireton formations of Alberta. *Bulletin of Canadian Petroleum Geology*, 1980, **28**, 234-410.
- (2) S.D.A. Anderson, C. D. Rokosh, J.G. Pawlowicz, H. Berhane and A. P. Beaton, 2010, Mineralogy, permeametry, mercury porosimetry, pycnometry and scanning electron microscope imaging of Duvernay and Muskwa Formations in Alberta: Shale Gas Data Release: ERCB/AGS Open File 830 Report, https://ags.aer.ca/document/OFR/OFR_2010_02.pdf (Accessed November 2018).
- (3) M.R. Yassin, M. Begum, and H. Dehghanpour, Organic shale wettability and its relationship to other petrophysical properties: A Duvernay case study. *International Journal of Coal Geology*, 2017, **169**, 74-91.
- (4) M.G. Fowler, L. D. Stasiuk, M. Hearn, and M. Obermajer, Devonian hydrocarbon source rocks and their derived oils in the Western Canada Sedimentary Basin. *Bulletin of Canadian Petroleum Geology*, 2001, **49**, 117-148.
- (5) N.R. Warner, T.M. Kresse, P.D. Hays, A. Down, J.D. Karr, R.B. Jackson, and A. Vengosh, A. (2013). Geochemical and isotopic variations in shallow groundwater in areas of the Fayetteville Shale development, north-central Arkansas, *Applied Geochemistry*, 2013, **35**, 207-220.

- (6) N. Shrestha, G. Chilkoor, J. Wilder, V. Gadhamshetty, and J.J. Stone, Potential water resource impacts of hydraulic fracturing from unconventional oil production in the Bakken Shale, *Water Res.*, 2017, **108**, 1-24.
- (7) J.S. Rosenblum, K.A. Sitterley, E.M. Thurman, I. Ferrer, and K.G. Linden,. Hydraulic fracturing wastewater treatment by coagulation-adsorption for removal of organic compounds and turbidity. *Journal of environmental chemical engineering*, 2016, **4(2)**, 1978-1984.
- (8) L.O. Haluszczak, A.W. Rose, and L.R. Kump, Geochemical evaluation of flowback brine from Marcellus gas wells in Pennsylvania, USA, *Appl. Geochem.*, 2013, **28**, 55-61.
- (9) E. Barbot, N.S. Vidic, K.B. Gregory, and R.D. Vidic, Spatial and temporal correlation of water quality parameters of produced waters from Devonian age shale following hydraulic fracturing, *Environ. Sci. Technol.*, 2013, **47**, 2562-2569.
- (10) C. He, X. Wang, W. Liu, E. Barbot, and R.D. Vidic, Microfiltration in the recycling of Marcellus Shale flowback water: solids removal and potential fouling of polymeric microfiltration membranes, *J. Membr. Sci.*, 2014c, **462**, 88-95.
- (11) T. Hayes and B.F. Severin, Barnett and Appalachian shale water management and reuse technologies, Report No. 08122-05, Research partnership to secure energy for America, 2012, https://edx.netl.doe.gov/dataset/barnett-and-appalachian-shale-water-management-and-reuse-technologies/resource_download/d167805d-9a16-40b8-b3fb-123ac3edab20, (Accessed November 2018)